SPECTRAL DIAGNOSTICS OF AN ACTIVE REGION OBSERVED BY THE SOLAR EUV ROCKET TELESCOPE AND SPECTROGRAPH (SERTS)

BHOLA DWIVEDI[1], ANITA MOHAN[1] and ROGER THOMAS[2]
[1]*Department of Applied Physics, Institute of Technology, Banaras Hindu University, Varanasi 221005, India*
[2]*Laboratory for Astronomy and Solar Physics, Code 680, NASA-Goddard Space Flight Center, Greenbelt, MD 20771, U.S.A.*

(Received 13 May 1997; accepted 28 November 1997)

Abstract. The EUV spectrum of a solar active region observed by SERTS-89 is used to estimate physical parameters such as electron density, elemental abundance and inhomogeneity in the emitting source. A total of 13 ions, namely, Ne IV–VI, Mg V–IX, Si VII–X and S X, are studied in the SERTS spectral range 170–450 Å, providing plasma diagnostics at temperatures between 10^5–10^6 K. Attention is called to results derived from ion pairs of different elements that are formed over similar temperature regimes, which allow special checks on the standard assumptions of spectral analyses. Some EUV lines, not originally reported in the SERTS-89 spectrum, are shown to have measureable intensities and are indicated for future observations.

1. Introduction

The physical properties of ionized plasma in the solar wind can be used to deduce conditions in the source region. *In situ* measurements or radio observations, for instance, provide information on nonthermal, transient, and sometimes catastrophic solar events. Nonetheless, the physical state of the solar plasma, e.g., electron density, temperature, and elemental abundance, is best inferred from an interpretation of its emissison-line spectrum (cf., Dwivedi, 1994a). Thus, spectroscopic diagnostics of the active corona are of major importance.

Thomas and Neupert (1994, hereafter referred as TN94), have reported a spectral catalogue of a solar active region based on observations made by the Solar EUV Rocket Telescope and Spectrograph (SERTS) on 5 May 1989. The SERTS combines spectral resolution good enough to resolve the typical thermal width of coronal lines with spatial imaging adequate to isolate many coronal structures. Spectral and spatial dimensions are completely separated, so that spectra of any solar feature may be obtained. Most of the line positions have been determined to a precision of 5 mÅ or better, representing the highest accuracy yet obtained for solar wavelengths throughout this spectral interval (170–450 Å). In addition, the radiometric calibration of the instrument has a relative uncertainty of no more than ±20% over its first-order range, providing accurate intensities of the observed emission lines. We use this spectral catalogue to estimate physical parameters in the active region.

Solar Physics **180:** 157–178, 1998.
© 1998 *Kluwer Academic Publishers. Printed in Belgium.*

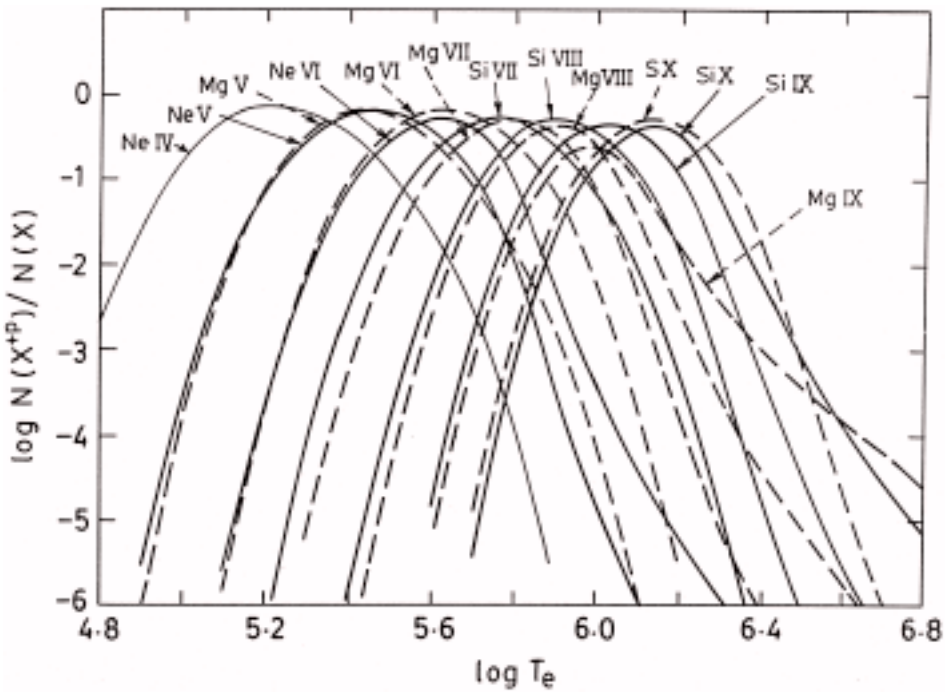

Figure 1. Ionization equilibrium curves for solar ions studied (from Arnaud and Rothenflug, 1985).

The observations and our method of analysis are briefly described in the following section. We present our results and offer some discussion in Section 3.

2. Observations and Method of Analysis

TN94 reported wavelengths and absolute intensities for 243 emission lines from a single active region observed by SERTS on 5 May 1989. Their imaged spectra were spatially averaged over a field of view $7'' \times 276''$ cutting through the centre of AR 5464 at S18 W45; measurements were made over the spectral range of 170 –450 Å with a resolution approaching 10 000. Although a recent re-evaluation of the absolute calibration scale for SERTS-89 indicates that all intensities reported in TN94 should be increased by a factor of 1.24, we will continue to use the original intensity scale in the present work to simplify comparisons with the published SERTS-89 catalogue. From this catalogue, we have selected several ions for our study, which are listed in Table I. These ions have their peak ionic concentrations in the temperature range $10^5 < T_{\max} < 10^6$ K as shown in Figure 1 from the ionization equilibrium calculations of Arnaud and Rothenflug (1985).

Table I
Column emission measure from the SERTS EUV spectrum of a solar active region

Ion	Wavelength (Å)	Intensity (ergs cm^{-2} s^{-1} sr^{-1})	$G_{\max}$	$[\Omega_{iu}/\omega_i]$	$A_{u\ell}/\Sigma A$	$1+\Sigma N_i/N_g$	$\int N_e^2\,\mathrm{d}s$	Remarks
Ne IV	357.889	7.8	$1.43-4$	1.65	0.66	3.49	$1.6+26$	
	421.592	4.3	$2.10-4$	0.80	1.00	($\beta=1$)	$1.0+26$	
Ne V	358.455	15.2	$2.67-4$	5.71	0.33	14.56	$4.0+26$	
	359.378	26.3	$2.65-4$	5.71	0.56	($\beta=0.95$)	$4.1+26$	
	416.208	24.2	$3.23-4$	6.33	1.00		$1.8+26$	
Mg V	351.117	13.1	$2.70-4$	0.73	0.41	2.78	$4.2+26$	
	353.084	10.4	$2.73-4$	1.25	0.75	($\beta=0.90$)	$1.1+26$	
	353.290[b]	10.1	$2.73-4$	0.73	0.255		$5.2+26$	blend Na VII
	403.296	9.0						
	354.162	11.3	$2.74-4$	0.73	0.34		$3.5+26$	
	355.339	6.2	$2.75-4$	1.25	0.25		$3.5+26$	
Ne VI	399.837	14.9	$3.22-4$	1.90	0.16	2.93	$5.5+26$	
	401.139	29.9	$3.23-4$	0.99	0.63	($\beta=0.80$)	$5.5+26$	
	401.936	84.6	$3.24-4$	1.90	0.83		$6.0+26$	
	403.296[b]	45.6	$3.25-4$	0.99	0.37		$1.4+27$	blend Mg VI
	433.161	7.5	$3.45-4$	0.73	0.37		$3.2+26$	
	435.632	9.8	$3.47-4$	0.73	0.63		$2.5+26$	
Mg VI	269.038	37.1	$2.56-4$	0.36	0.73	3.01	$1.2+26$	
	270.401	59.1	$2.57-4$	0.71	0.70	($\beta=0.90$)	$9.9+26$	
	349.162	55.2	$3.50-4$	0.50	0.81		$1.0+27$	self-blend
				0.67	0.04		$1.1+27$	
	387.955	8.2	$3.85-4$	0.67	0.14		$6.8+26$	
	399.275	9.3	$3.95-4$	0.27	1.00		$2.8+26$	

Table I
Continued

Ion	Wavelength (Å)	Intensity (ergs cm^{-2} s^{-1} sr^{-1})	$G_{\max}$	$[\Omega_{iu}/\omega_i]$	$A_{u\ell}/\Sigma A$	$1+\Sigma N_i/N_g$	$\int N_e^2\,ds$	Remarks
	400.668	16.2	3.97 − 4	0.51	1.00		2.6 + 26	
	403.296[b]	45.6	4.00 − 4	0.77	1.00		4.8 + 26	blend Ne VI
Si VII	275.377	105.0	2.69 − 4	0.56	0.75	2.31 ($\beta = 0.79$)	1.7 + 27	
Mg VII	277.045[b]	85.1	2.70 − 4	2.55	0.33		3.1 + 27	blend Si VIII
	278.407	114.0	2.72 − 4	2.55	0.56	9.75	2.5 + 27	
	363.753	76.4	3.29 − 4	1.37	0.33	($\beta = 0.78$)	8.3 + 26	
	319.023[b]	11.2	3.01 − 4	0.49	0.99		4.9 + 27	blend Ni XV
	365.210	23.2	3.40 − 4	0.47	0.23		2.5 + 27	self-blend
				0.75	0.28		1.1 + 27	
				0.15	1.00		1.8 + 27	
	367.675	46.2	3.50 − 4	0.47	0.78		3.0 + 27	self-blend
				0.75	0.40		1.3 + 27	
	429.132	10.9	3.63 − 4	1.02	0.59		6.4 + 26	
	431.141	9.2	3.64-4	1.02	0.39		8.3 + 26	
	431.288	17.6	3.64 − 4	1.44	0.80		5.4 + 26	
	434.917	27.9	3.65-4	1.80	1.00		5.5 + 26	
Si VIII	276.850	65.6	2.92 − 4	0.18	0.82	1.87	2.6 + 27	
	277.045[b]	85.1	2.93 − 4	0.18	0.07		4.0 + 28	blend Mg VII
	314.345	54.1	3.16 − 4	0.18	1.00	($\beta = 0.70$)	1.8 + 27	
	316.220	88.7	3.17 − 4	0.34	1.00		1.6 + 27	
	319.839	113.0	3.18 − 4	0.52	1.00		1.3 + 27	
Mg VIII	311.778[b]	79.1	2.67 − 4	1.56	0.16		4.2 + 27	blend Ni XV
	313.736	80.3	2.68 − 4	0.79	0.58	2.98	2.3 + 27	

Table I
Continued

Ion	Wavelength (Å)	Intensity (ergs cm^{-2} s^{-1} sr^{-1})	$G_{\max}$	$[\Omega_{iu}/\omega_i]$	$A_{u\ell}/\Sigma A$	$1+\Sigma N_i/N_g$	$\int N_e^2\,\mathrm{d}s$	Remarks
	315.024	253.0	$2.69-4$	1.56	0.84	($\beta=0.63$)	$2.6+27$	
	317.008	57.5	$2.70-4$	0.79	0.42		$2.3+27$	
	339.000	53.8	$2.80-4$	0.53	0.57		$2.4+27$	
	430.445	40.3	$3.14-4$	0.59	0.85		$1.2+27$	
	436.726	67.5	$3.15-4$	0.82	1.00		$1.3+27$	
Si IX	258.095	49.7	$2.49-4$	0.54	1.00	7.53	$2.2+27$	
	290.693	33.2	$2.66-4$	0.91	0.31	($\beta=0.75$)	$2.9+27$	
	292.801	70.6	$2.67-4$	0.30	0.20		$1.4+28$	self-blend
				0.91	0.30		$3.3+27$	
	296.137	208.0	$2.68-4$	0.30	0.80		$1.6+28$	self-blend
				0.91	0.38		$3.8+27$	
	341.974	29.4	$2.87-4$	0.70	0.62		$1.9+27$	
	344.958	17.3	$2.87-4$	0.70	0.62		$1.9+27$	
	345.130	70.9	$2.87-4$	0.98	0.83		$2.4+27$	
	349.872	140.0	$2.88-4$	0.24	1.00		$1.4+28$	self-blend
				0.98	0.17		$2.9+27$	
Mg IX	368.063	1070.0	$1.73-4$	1.59	1.00	1.11	$6.5+27$	
	439.173	9.4	$1.85-4$	0.06	0.26	($\beta=0.60$)	$6.8+27$	
	441.221	7.7	$1.85-4$	0.04	0.34		$6.8+27$	
	443.371	5.6	$1.86-4$	0.04	0.25		$6.8+27$	
	443.956	19.6	$1.86-4$	0.06	0.74		$4.9+27$	
	448.279	4.7	$1.87-4$	0.04	0.41		$3.5+27$	
Si X	253.808	207.0	$2.21-4$	0.68	0.28	1.97	$7.9+27$	
	256.323	1580.0	$2.22-4$	0.45	0.71		$2.9+28$	blend He II

Table I
Continued

Ion	Wavelength (Å)	Intensity (ergs cm^{-2} s^{-1} sr^{-1})	$G_{\max}$	$[\Omega_{iu}/\omega_i]$	$A_{u\ell}/\Sigma A$	$1+\Sigma N_i/N_g$	$\int N_e^2\,\mathrm{d}s$	Remarks
	258.368	377.0	$2.23-4$	0.68	0.72	($\beta = 0.71$)	$5.6+27$	
	261.049	140.0	$2.24-4$	0.45	0.30		$7.8+27$	
	271.992	131.0	$2.28-4$	0.30	0.92		$3.6+27$	
	277.268	114.0	$2.29-4$	0.30	0.08		$3.6+28$	
	347.406	210.0	$2.49-4$	0.39	0.93		$5.1+27$	
	356.027	218.0	$2.54-4$	0.39	0.07		$5.5+27$	
				0.30	1.00		$5.9+27$	
S X	259.495	123.0	$2.81-4$	0.26	1.00	1.32	$7.3+27$	
	264.221	96.3	$2.84-4$	0.40	1.00	($\beta = 0.80$)	$3.8+27$	

Note: $1.43-4$ means 1.43×10^{-4}; [b] indicates blending of the line.

Following Widing, Feldman, and Bhatia (1986), the total line intensity emitted in a radiative transition from upper level u to lower level ℓ by a cm^2 plasma column on the Sun along the line of sight from Earth is given by

$$I(\lambda_{u\ell}) = \frac{1.13 \times 10^{-22}}{\lambda\ (\mathrm{cm})} \left[\frac{\Omega_{iu}}{\omega_i}\right] \frac{1}{1 + \sum\limits_i N_i/N_g} \frac{A_{u\ell}}{\sum\limits_\ell A_{ul}} \times$$

$$\times \frac{N(X)}{N(H)} \int G(T) N_e^2\, \mathrm{d}s \quad \text{ergs cm}^{-2}\ \text{s}^{-1}\ \text{sr}^{-1}\ . \tag{1}$$

In this expression, $N(H)/N_e = 0.83$ has been adopted and

$$\left[\frac{\Omega_{iu}}{\omega_i}\right] = \frac{\Omega_{gu}}{\omega_g} + \frac{N_1}{N_g}\frac{\Omega_{1u}}{\omega_1} + \frac{N_2}{N_g}\frac{\Omega_{2u}}{\omega_2} + \cdots\ ;$$

N_i and N_g are the number density in level i and ground state g, respectively, Ω_{iu} is the collision strength, and ω_i is the statistical weight of the initial level. $N(X)/N(H)$ is the elemental abundance relative to hydrogen, which may not be constant in the solar atmosphere, and

$$G(T) = N(X^{+p})/N(X)\ e^{-\Delta E/kT}/T^{1/2}\ , \tag{2}$$

where $N(X^{+p})/N(X)$ is the ionization fraction at temperature T, which has been adopted from Arnaud and Rothenflug (1985). The averaged value of $G(T)$ has been estimated following Jordan and Wilson (1971) to a constant logarithmic width of $\Delta \log T = \log T_{\mathrm{max}} \pm 0.15$ which corresponds to temperature limits of $1.412 T_{\mathrm{max}}$ and $0.708 T_{\mathrm{max}}$, so that

$$\langle G(T) \rangle = \int G(T)\ \mathrm{d}T/0.078 T_{\mathrm{max}} = \beta G_{\mathrm{max}}\ , \tag{3}$$

where G_{max} is the maximum value of $G(T)$ and β is the normalizing constant.

Adopting Equation (3) for the average value of $G(T)$ and removing it from the integral in Equation (1), we get the final expression

$$I(\lambda_{u\ell}) = \frac{1.13 \times 10^{-22}}{\lambda\ (\mathrm{cm})} \left[\frac{\Omega_{iu}}{\omega_i}\right] \frac{\beta G_{\mathrm{max}}}{1 + \sum\limits_i N_i/N_g} \frac{A_{u\ell}}{\sum\limits_\ell A_{ul}} \times$$

$$\times \frac{N(X)}{N(H)} \int N_e^2\, \mathrm{d}s \quad \text{ergs cm}^{-2}\ \text{s}^{-1}\ \text{sr}^{-1}\ . \tag{4}$$

Atomic data have been taken from various published sources for the different ions, and most of them have been discussed in our previous studies.

The proceedings of an atomic data assessment meeting held in March 1992 in Abingdon has been compiled in a special issue of *Atomic Data and Nuclear Data*

Tables **57**, Nos. 1/2 (1994). We have adopted this data-set in our present study. Consequently, our previous studies wherever required have been updated in the light of recommended atomic data for Be-like ions (Mg IX) by Berrington (1994), for B-like ions (Ne VI, Mg VIII, Si X) by Sampson, Zhang, and Fontes (1994) and by Zhang, Graziani, and Pradhan (1994), for C-like ions (Ne V, Mg VII, Si IX) by Monsignori Fossi and Landini (1994), for N-like ions (Ne IV, Mg VI, Si VIII, S X) by Kato (1994), and for O-like ions (Mg V, Si VII) by Lang and Summers (1994). Values of $G_{\max}$ together with other factors appearing in Equation (4) are tabulated for each spectral line in Table I, along with derived values of $\int N_e^2 \, \mathrm{d}s$. Level populations have been.estimated for an adopted electron density of 10^{10} cm^{-3}. The elemental abundances have been taken from Meyer (1985).

There are four lines from ions in our study that are predicted to be several orders of magnitude fainter than observed by SERTS-89 if due to the transitions given for them in TN94 (Young, 1996), namely Mg V 376.625 Å, Mg VI 319.726 Å, Si VIII 338.375 Å, and Si X 292.251 Å. These spectral features are clearly dominated by emission from other transitions than the ones suggested by TN94, and will not be discussed further here.

With the above exceptions, Table I lists all the lines from ions in our study that were reported by TN94 as being measured in the SERTS-89 averaged active region spectrum. However, we have found a number of additional lines from these ions in the SERTS spectral range that should be relatively intense under certain conditions, and thus might be measureable with improved instrumental performance, with deeper exposures, or with observations of a brighter emitting region. These additional lines are presented in Table II. For some of them, marginal detections have been derived from the original SERTS-89 data, and are also indicated in Table II (see remarks with blend, mask and line intensity from SERTS-89). These candidates were suggested either by reports from earlier space observations, such as Malinovsky and Héroux (1973), Behring *et al.* (1976), and Vernazza and Reeves (1978), or by our own theoretical calculations using a representative spherically-symmetric model atmosphere for the quiet Sun. These new identifications have further been endorsed by Young, Landi, and Thomas (1998).

3. Results and Discussion

The computed values of the column emission measure listed in Table I are plotted in Figure 2 as a function of $T_{\max}$ for unblended lines. In our analysis, there are six pairs of ions whose ionization fractions strongly overlap one other, as can be seen in Figure 1 (the one unpaired ion being Ne IV). For instance, the curves for Ne V and Mg V ions are nearly identical, both having peak values at about $T_{\max} = 2.8 \times 10^5$ K. One can, therefore, assume that lines from Ne V and Mg V ions originate essentially from the same emitting layers in the Sun's atmosphere. A similar argument can be made for the other pairs of ions, namely Ne VI–Mg VI, Si VII–Mg VII, Si VIII–

Table II
Additional EUV lines with potentially observable intensities in the SERTS spectral range

Ion	Wavelength (Å)	Transition		Remarks	
		Configuration	Term	Predicted intensities for the quiet Sun (ergs cm^{-2} s^{-1} sr^{-1})	Measured SERTS-89 intensity*
Ne IV	358.721	$2s^2\,2p^3 - 2s2p^4$	$^2D^0_{5/2} - ^2P_{3/2}$	1.70	blend Fe XI 358.67
	388.218	$2s^2\,2p^3 - 2s2p^4$	$^2P^0_{3/2} - ^2P_{3/2}$	0.48	1.4 ± 0.8
Ne V	365.61	$2s^2\,2p^2 - 2s2p^3$	$^1D_2 - ^1P^0_1$	6.3	blend Fe X 365.57
Mg V	276.582	$2s^2\,2p^4 - 2s2p^5$	$^1D_2 - ^1P^0_1$	3.4	22.4 ± 12.3
	352.200	$2s^2\,2p^4 - 2s2p^5$	$^3P_1 - ^3P^0_0$	1.2	4.3 ± 3.1
Mg VI	291.348	$2s^2\,2p^3 - 2s2p^4$	$^2P^0_{1/2} - ^2P_{1/2}$	0.53	10.3 ± 6.3
	293.124	$2s^2\,2p^3 - 2s2p^4$	$^2P^0_{3/2} - ^2P_{3/2}$	1.26	14.0 ± 8.1
	314.676	$2s^2\,2p^3 - 2s2p^4$	$^2P^0_{3/2} - ^2S_{1/2}$	0.93	15.8 ± 6.3
				Listed in TN94 as unidentified	
	387.787	$2s^2\,2p^3 - 2s2p^4$	$^2P^0_{1/2} - ^2D_{3/2}$	0.58	3.8 ± 1.5
Si VII	217.826	$2s^2\,2p^4 - 2s2p^5$	$^1D_2 - ^1P^0_1$	3.5	2nd order blend Ne VI 435.63
	272.641**	$2s^2\,2p^4 - 2s2p^5$	$^3P_2 - ^3P^0_1$	5.9	19.8 ± 9.8
	274.175	$2s^2\,2p^4 - 2s2p^5$	$^3P_1 - ^3P^0_0$	4.1	blend Fe XIV 274.21
	275.665	$2s^2\,2p^4 - 2s2p^5$	$^3P_1 - ^3P^0_1$	3.4	17.6 ± 13.8
	276.839	$2s^2\,2p^4 - 2s2p^5$	$^3P_0 - ^3P^0_1$	4.4	blend Si VIII 276.85
	278.445	$2s^2\,2p^4 - 2s2p^5$	$^3P_1 - ^3P^0_2$	6.3	blend Mg VII 278.41
Mg VII	276.145	$2s^2\,2p^2 - 2s2p^3$	$^3P_0 - ^3S^0_1$	2.9	21.9 ± 9.2
	280.744	$2s^2\,2p^2 - 2s2p^3$	$^1D_2 - ^1P^0_1$	3.6	9.4 ± 7.5

Table II
Continued

Ion	Wavelength (Å)	Transition		Remarks	
		Configuration	Term	Predicted intensities for the quiet Sun (ergs cm^{-2} s^{-1} sr^{-1})	Measured SERTS-89 intensity*
Si VIII	214.756	$2s^2\,2p^3 - 2s2p^4$	$^2D^0_{3/2} -^2 P_{1/2}$	3.2	2nd order blend Fe XIV 429.54
	216.918	$2s^2\,2p^3 - 2s2p^4$	$^2D^0_{5/2} -^2 P_{3/2}$	8.8	2nd order 30.6 ± 23.5
Mg VIII	335.230	$2s^2\,2p - 2s2p^2$	$^2P^0_{1/2} -^2 S_{1/2}$	7.0	masked by Fe XVI 335.40
Si IX	223.72	$2s^2\,2p^2 - 2s2p^3$	$^3P_0 -^3 S^0_1$	6.5	2nd order blend Fe XIV 447.34
	225.033	$2s^2\,2p^2 - 2s2p^3$	$^3P_1 -^3 S^0_1$	18.6	data gap
	227.007	$2s^2\,2p^2 - 2s2p^3$	$^3P_2 -^3 S^0_1$	29.8	data gap
S X	180.72	$2s^2\,2p^3 - 2s2p^4$	$^2D_{5/2} -^2 P_{3/2}$	1.5	blend Si XI 361.41
	228.70	$2s^2\,2p^3 - 2s2p^4$	$^2D^0_{5/2} -^2 D_{5/2}$	1.8	data gap
	257.16	$2s^2\,2p^3 - 2s2p^4$	$^4S^0_{3/2} -^4 P_{1/2}$	5.8	28.8 ± 17.8

*In ergs cm^{-2} s^{-1} sr^{-1} on the old absolute scale; to place them on the revised scale, they need to be multiplied by a factor of 1.24.
**Observed at 272.555 ± 0.002 Å.

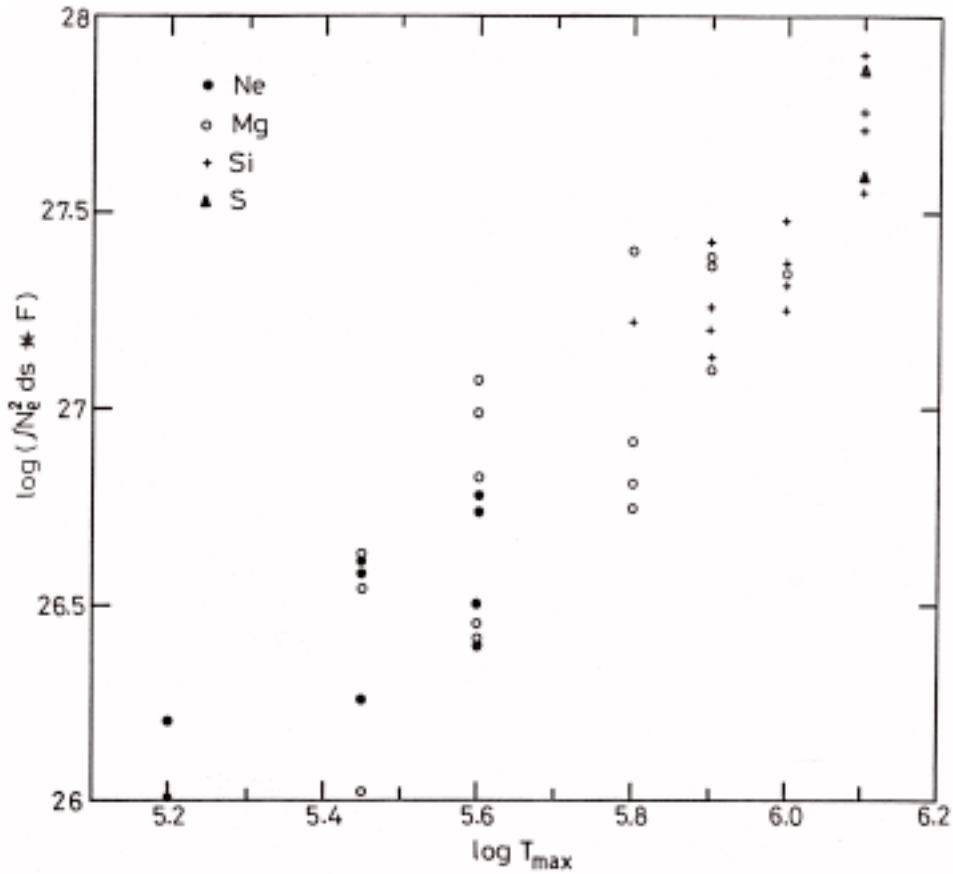

Figure 2. The column emission measure as a function of T_{max}.

Mg VIII, Si IX–Mg IX, and finally, Si X–S X. This then provides a special opportunity to compare emission measure obtained from atomic calculations, making use of assumed elemental abundances and the measured line intensities. Alternatively, by forcing the emission measures to agree, the corresponding relative elemental abundances can be estimated. If EUV observations from different regions of the solar atmosphere are available, one can readily study the relative elemental abundances in different solar features and their possible variations, making use of the tabulated values of atomic calculations listed in Table I.

For the SERTS-89 observations averaged over a solar active region, Table I shows that the column emission measures for different spectral lines from each such pair of ions are found to be within the experimental uncertainty in the measured intensity of about 30% or so for most of the lines. However, they seem to differ by a factor of 2 or even more for some of the lines. Results from the six ion pairs are described individually below.

3.1. Ne V and Mg V ions

Ne V λ416.20/λ358.45 and λ416.20/λ359.37 theoretical line ratios are known to be density-sensitive in the range 10^8–10^{10} cm^{-3}. Dwivedi and Mohan (1995a) estimated an electron density of 5.6×10^8 cm^{-3} from these line ratios making use of the SERTS-89 observations. This rather low value of electron density in the active region is not explained at present. Unfortunately, the six Mg V lines reported by TN94 offer no pairs that can be used for a direct density check. However, the previously unreported Mg V λ276.58 line is involved in a number of density-sensitive line ratios, including λ276.58/λ351.11, λ276.58/λ353.08, λ276.58/λ354.16, and λ276.58/λ355.33 which are shown in Figure 3. The figure also shows measured values of these ratios based on a new marginal detection of Mg V λ276.58 in the SERTS-89 active region spectrum at an intensity of 22.4 ± 12.3 ergs cm^{-2} s^{-1} sr^{-1} (Table II). With one exception, all of these measured ratios are compatible with an electron density $\geq 2.0 \times 10^9$ cm^{-3}. The exception is λ276.58/λ353.08, where the measured 1-σ lower limit is still higher than the maximum predicted theoretical value.

Recently, Dwivedi and Mohan (1995a) reported several Ne V/Mg V density-sensitive line ratios for density measurements, λ416.20/λ355.33, λ416.20/λ354.16, λ416.20/λ351.11, λ416.20/λ353.08, λ359.37/λ276.58, and λ358.45/λ276.58.

We now also find λ358.45/λ354.16, λ359.37/λ354.16, λ358.45/λ355.33, and λ359.37/λ355.33 Ne V/Mg V line ratios to be density-insensitive as shown in Figure 4. These provide a unique opportunity to estimate the Ne/Mg relative elemental abundance, which is found to be 1.15 in the active region observed by SERTS-89. Element abundance of Ne and Mg with respect to hydrogen are 3.5×10^{-5} and 3.7×10^{-5}, respectively (Meyer, 1985). Widing and Feldman (1989) report a value of 0.64 in the active region for Ne/Mg abundance ratio and its variation from 0.8 to 1.5 in active region loops and flare loops. Using an average value of 0.8 and 1.5, which means $\mathrm{Ne/Mg} = 1.15$, which may be a reasonable value for the active region (not completely representative of non-flaring active regions) and the SERTS-89 observations, Dwivedi and Mohan (1995b) estimated electron density of about 5×10^9 cm^{-3}.

Another significant point to add is the possible FIP-effect in operation. Thus Ne V/Mg V density-insensitive line ratios (cf., Figure 4) call for a more careful study as to whether FIP-effect is a real one or an artifact of several complexities presently not fully understood.

3.2. Ne VI and Mg VI ions

Ne VI line ratios in the SERTS spectral range are not density-sensitive. For instance, Ne VI λ399.83/λ401.93 line ratio is insensitive of density variation from 10^8 to 10^{12} cm^{-3} giving a constant value of 0.2 which is in excellent agreement with the SERTS-89 observation of 0.18. Mg VI density-sensitive line ratios λ387.95/λ399.27

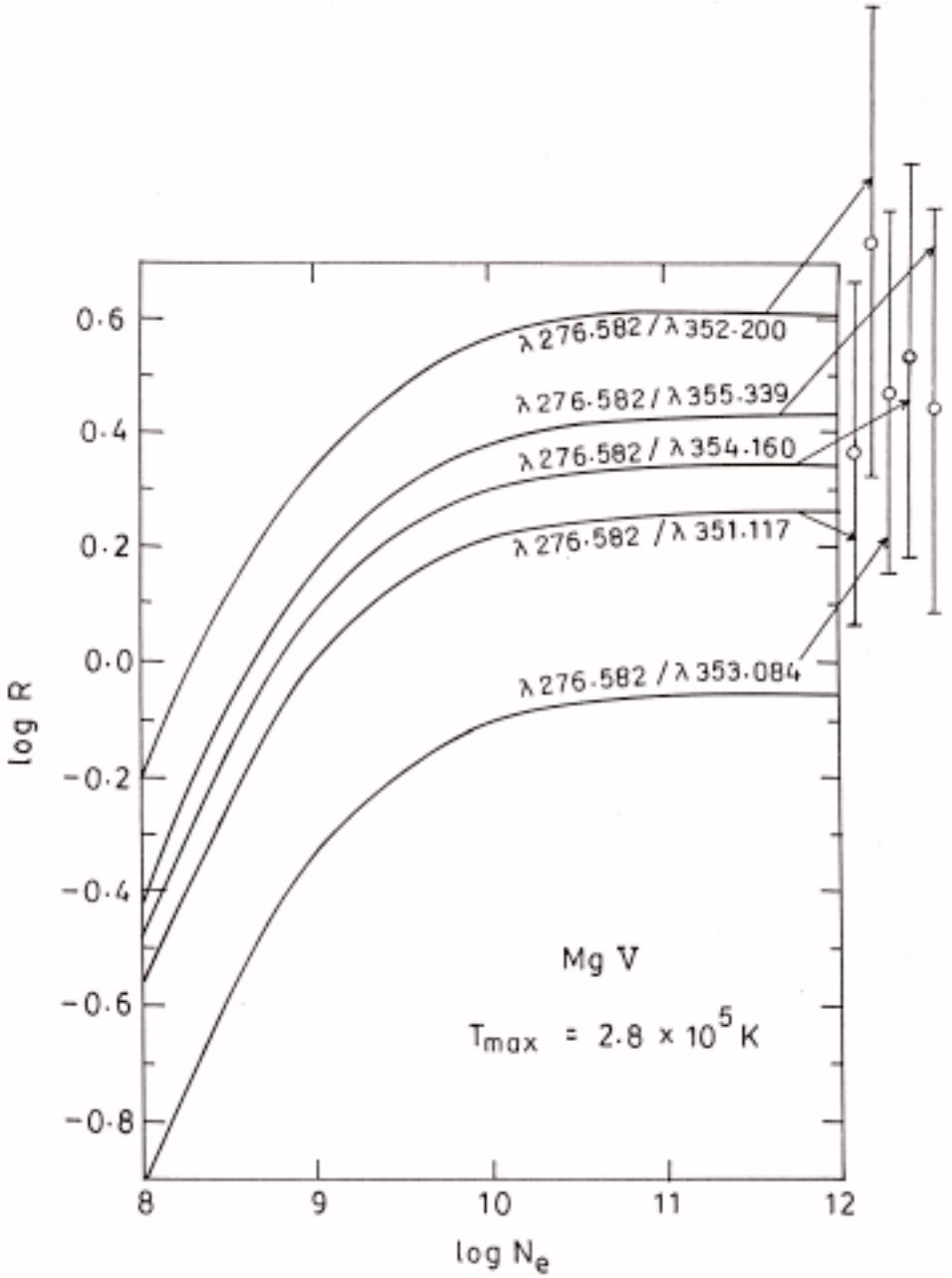

Figure 3. Mg V theoretical line-ratio curves at $T_{max} = 2.8 \times 10^5$ K as a function of electron density. The marginal detection of the line λ276.58 is given in Table II. The SERTS-89 observed intensity ratios in the active-region spectrum are shown by circles and error bars.

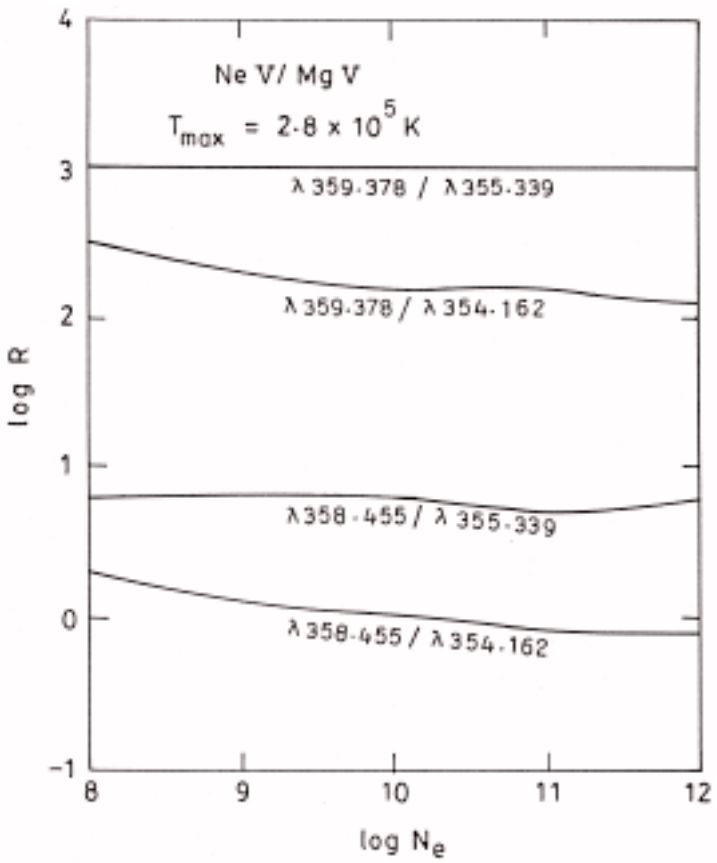

Figure 4. Ne V/Mg V density-insensitive line ratios at $T_{max} = 2.8 \times 10^5$ K.

and λ387.95/λ400.66 do not explain the observed line intensity ratios. These density-sensitive line ratios are shown in Figure 5. However, the observation from SERTS-89 for both the line ratios do not fall on the theoretical line ratio curves (cf., Table I) and we do not know at present the reason for such a disagreement between the theory and observation. Dwivedi and Mohan (1995b), however, have studied Ne VI/Mg VI line ratios for density determination as well as relative element abundances. Using Ne/Mg = 1.15 and line intensities (cf., Table I), they have estimated electron densities from several theoretical density-sensitive line ratio curves involving Ne VI λ399.83, λ401.13, λ401.93 and Mg VI λ399.27, λ400.66, λ403.29 lines. The inferred densities from this study vary from 2×10^{10} to 8×10^{10} cm^{-3}.

3.3. Si VII AND Mg VII IONS

Only one line of Si VII, namely λ275.37 was reported by TN94. Our calculations show that λ217.83, λ272.64, and λ275.66 should also be reasonably strong (cf.,

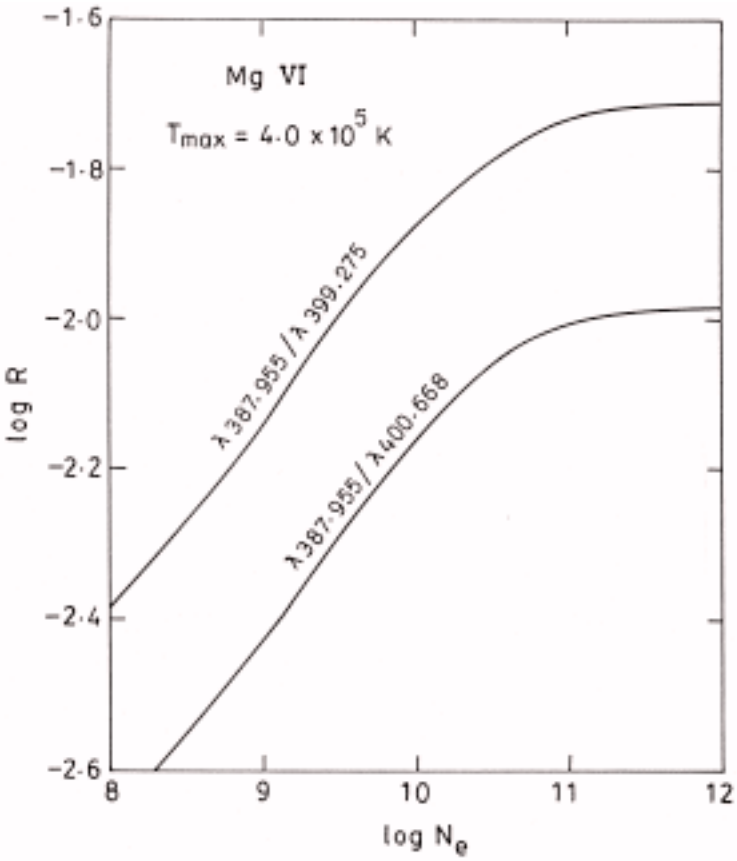

Figure 5. Mg VI density-sensitive line ratios at $T_{max} = 4 \times 10^5$ K.

Table II), and that the ratios λ217.83/λ275.37 and λ272.64/λ217.83 could be useful density diagnostics (Dwivedi, 1996). SERTS observes 217.83 Å in second order where it is blended with Ne VI 435.63 Å but this line might effectively be studied by instruments such as SOHO/CDS which observe it directly in first order. Table II shows possible detections of Si VII 272.64 Å and 275.66 Å in the SERTS-89 spectrum; other potentially observable Si VII lines are affected by blends, however.

Dwivedi (1994b) presented recent calculations of Mg VII λ319.02/λ434.91 ratio, but found that the SERTS-89 observation does not fall on the density-sensitive theoretical curve. This is to be expected for relatively high-temperature plasmas, due to known blending with Ni XV 319.03 Å.

3.4. Si VIII and Mg VIII ions

Dwivedi and Mohan (1995b) found at least three density-sensitive Si VIII line ratios very well observed by SERTS-89 and suitable for active region diagnostics,

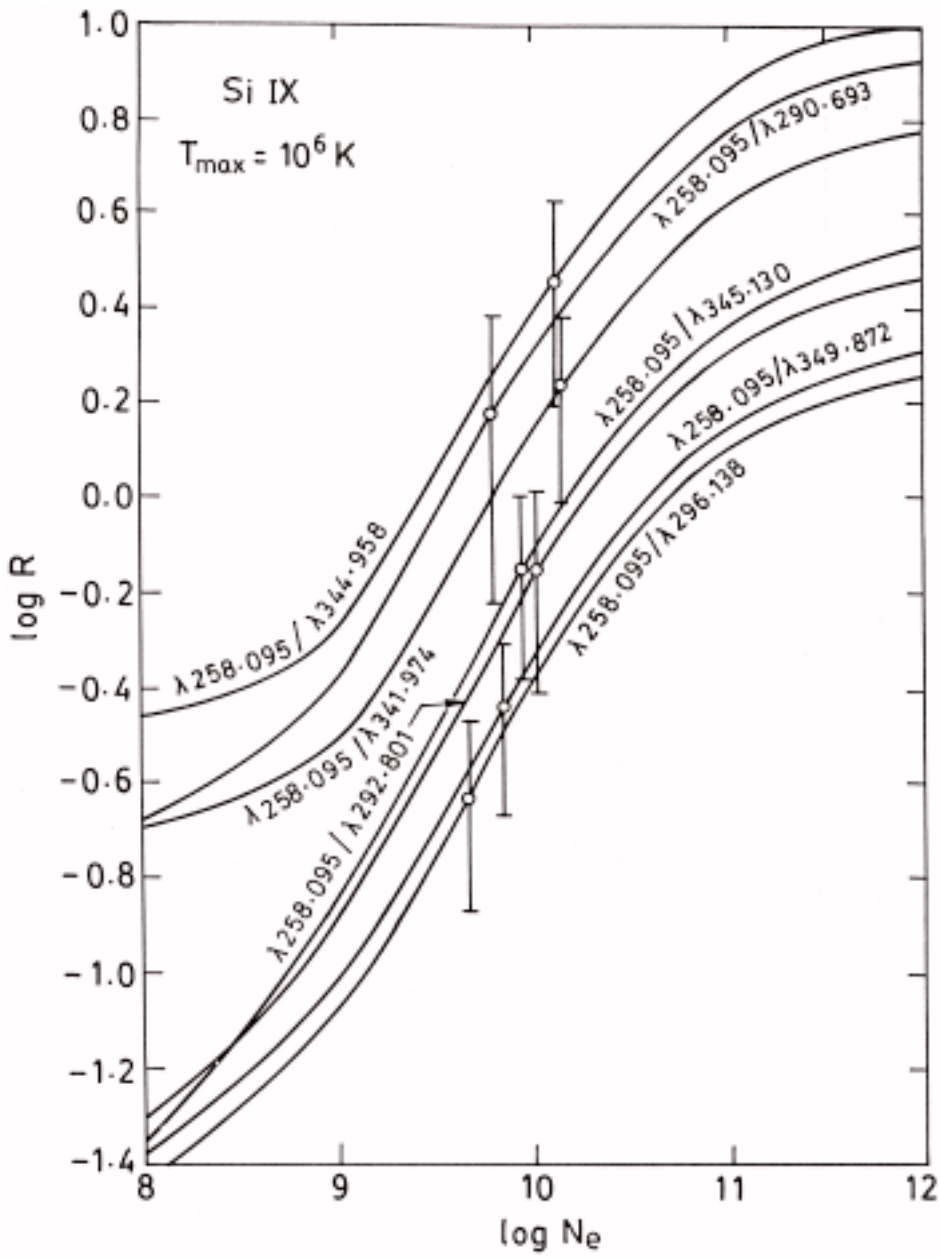

Figure 6. Si IX density-sensitive line ratios at $T_{max} = 10^6$ K. The SERTS-89 observed intensity ratios in the active region spectrum are shown by circles and error bars.

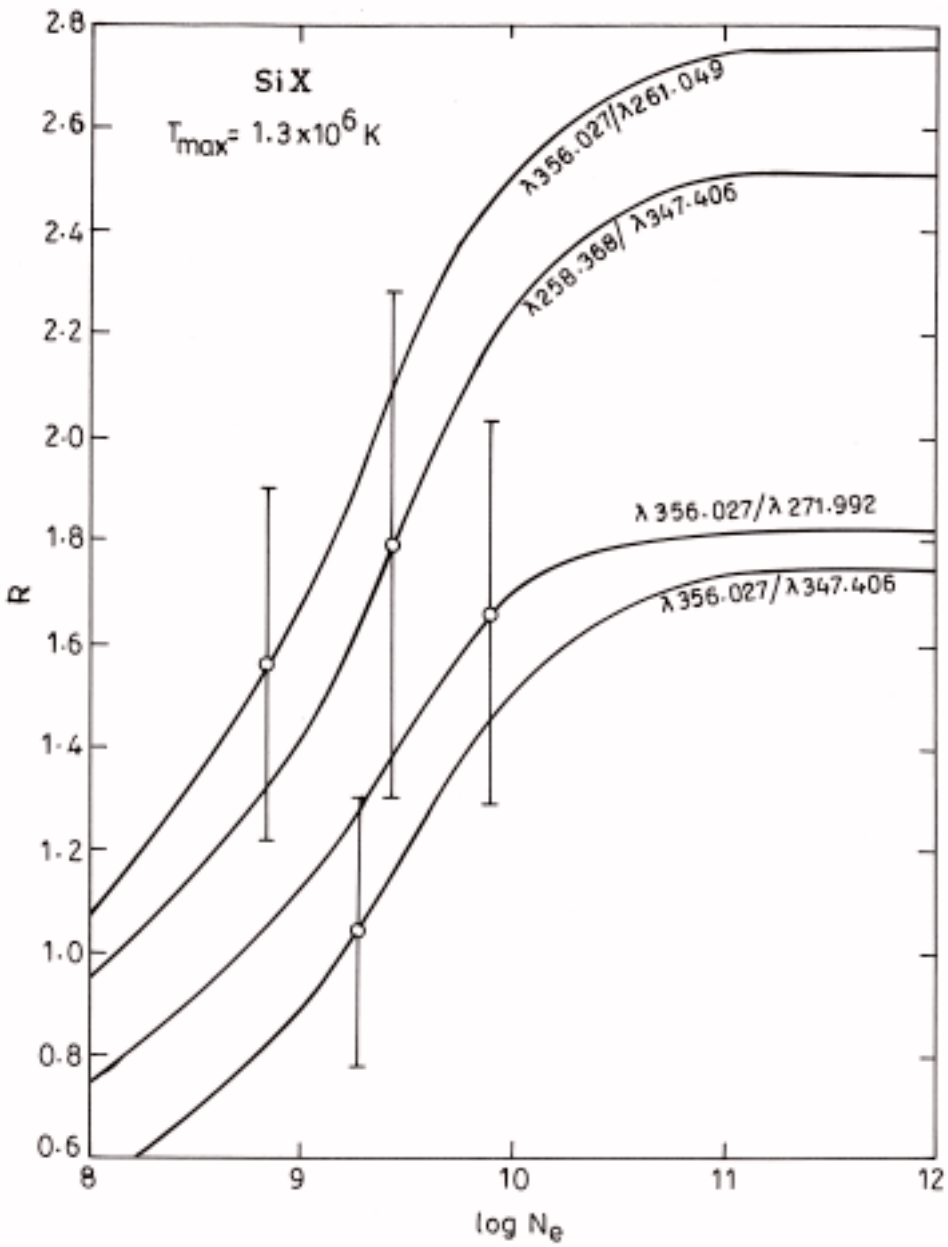

Figure 7. Si X density-sensitive line ratios at $T_{max} = 1.3 \times 10^6$ K. The SERTS-89 observed intensity ratios in the active region spectrum are shown by circles and error bars.

namely λ276.85/λ314.34, λ276.85/λ316.22, and λ276.85/λ319.83. They provided electron density estimates of 3×10^{10}, 4.5×10^{10}, and 8×10^{10} cm^{-3}, respectively. However, Si VIII λ276.85 line is blended with Si VII λ276.839 line. Our theoretical

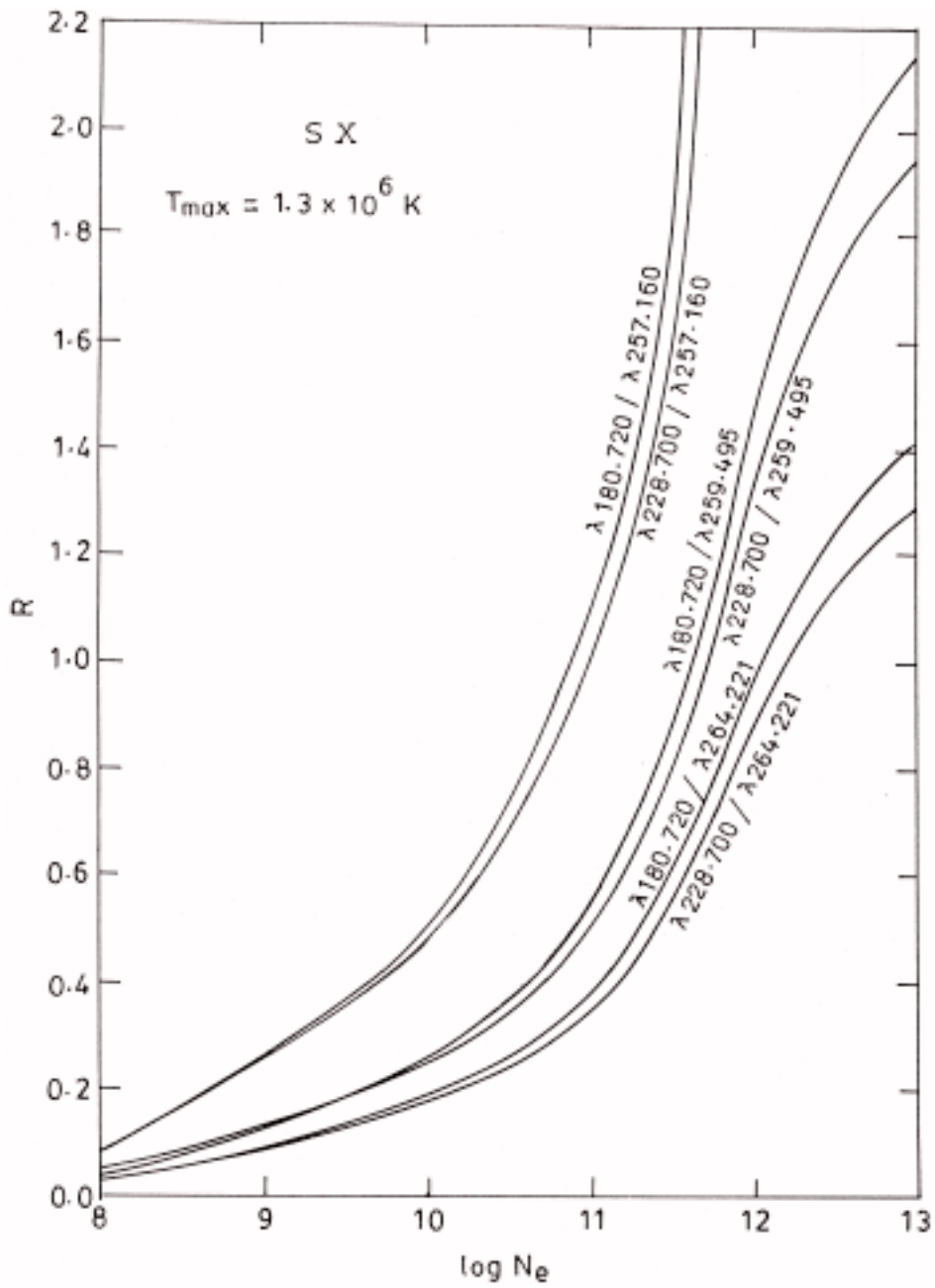
S X
Tmax = 1.3 x 10^6 K
λ 180.720 / λ 257.160
λ 228.700 / λ 257.160
λ180.720 / λ259.495
λ 228.700 / λ 259.495
λ180.720 / λ264.221
λ 228.700 / λ 264.221
R
log Ne
2.2
2.0
1.8
1.6
1.4
1.2
1.0
0.8
0.6
0.4
0.2
0.0
8
9
10
11
12
13

Figure 8a.

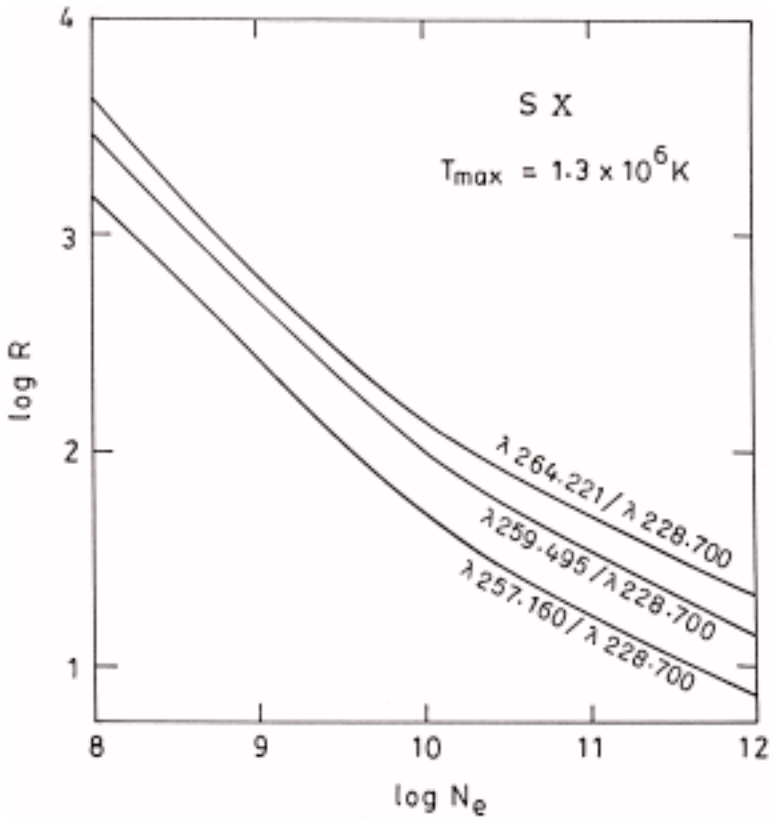

Figure 8b.

Figure 8a–b. S X density-sensitive line ratios at $T_{max} = 1.3 \times 10^6$ K.

calculations using a representative spherically symmetric model atmosphere for the quiet Sun suggest that both these lines have almost the same line intensity, i.e., 0.55×10^{-3} ergs cm^{-2} s^{-1}. This result would suggest that line intensity reported in TN94 for Si VIII λ276.85 in the active region should probably have half of its intensity. Accordingly, after taking account of a blending problem this provides electron density estimates of 3.2×10^9, 4.7×10^9, and 8.4×10^9 cm^{-3} instead. The well known density-sensitive Mg VIII λ430.44/λ436.72 line ratio, however, saturates at active region densities and so is not suitable for probing them.

3.5. Si IX and Mg IX ions

The SERTS-89 spectrum for Si IX contains a number of line-pairs that are good candidates for density measurement. We show in Figure 6 the dependence on electron density of several such line ratios at $T_{max} = 10^6$ K. The circles and error bars in this figure refer to the line intensity values reported by TN94.

An electron density of 10^{10} cm^{-3} for this active region seems to provide an excellent match of observed to predicted intensities for all of these lines. On the other hand, we do not find any good Mg IX line-pair for density measurement in the SERTS range. However, several density-sensitive Si IX/Mg IX line ratios have recently been reported by Mohan and Dwivedi (1996). These ratios include λ258.10/λ443.37, λ258.10/λ441.22, λ258.10/λ448.28, λ258.10/λ439.47, λ258.10/λ443.96, and λ258.10/λ368.06. From these line ratios, the density variation within the error limits is estimated to be from 10^9 cm^{-3} to 10^{10} cm^{-3} in the upper transition region and the lower corona, using a value of Si/Mg $= 1.05$.

3.6. Si X and S X ions

In the SERTS spectral range, Si X λ356.02/λ261.04, λ258.36/λ347.40, λ356.02/λ271.99, and λ356.02/λ347.40 form density-sensitive ratios as shown in Figure 7. The figure also shows the corresponding measured values as derived from SERTS-89 observations. All of the measured ratios are compatible with an electron density of $2-8\times10^9$ cm^{-3} which is in agreement with results reported by Young, Landi, and Thomas (1998). The ratio of the two S X lines reported by TN94 does not vary with density. However, we find that S X ratios of λ264.22/λ228.64, λ259.49/λ228.64, λ257.16/λ228.64, λ180.78/λ259.49, λ180.78/λ264.22, λ180.78/λ257.16, λ228.70/λ257.16, λ228.70/λ259.49, and λ228.70/λ264.22 would be good density diagnostics. These line ratio curves are shown in Figures 8(a) and 8(b). SERTS observes 180.78 Å in second order where it is blended with Si XI λ361.41 Å and has a gap in its coverage between 225–235 Å so can not measure 228.64 Å. There was a marginal detection of S X 257.16 Å by SERTS-89, as shown in Table II.

3.7. Electron density and filling factor

In order to obtain a value of N_e from the emission measure, we make the use of well-observed EUV lines for which we have

$$\int N_e^2 \, \mathrm{d}s \simeq 10^{27} \, .$$

If we take account of filling factor (F), Equation (4) will evidently become:

$$I = \text{constant} \times \text{atomic parameters} \frac{N(X)}{N(H)} \int N_e^2 \, \mathrm{d}s \; F \quad \text{ergs cm}^{-2} \text{ s}^{-1} \text{ sr}^{-1} \, ,$$

i.e.,

$$F \int N_e^2 \, \mathrm{d}s \simeq F N_e^2 \Delta s = 10^{27} \, .$$

Now, from density-sensitive line ratios, we have

$$N_e = 10^{10}\ \mathrm{cm}^{-3}$$

and we get

$$F\Delta s = 10^7\ \mathrm{cm}\ .$$

If we force the emission measure to agree for an expected path length of 10^9 cm, we get the filling factor of 0.01.

In conclusion, the study of density and temperature inhomogeneities in any solar structure call for both theoretical (e.g., Brown *et al.*, 1991) and observations at higher spatial resolution. In this paper we have primarily been confined to presenting potential application of the line-ratio diagnostics for a total of 13 ions with new identifications of several EUV lines from these ions, apart from presenting the derived values of $\int N_e^2\ \mathrm{d}s$ and a brief discussion on density inhomogeneity. A future paper will utilize this information to infer information about the solar atmosphere.

Acknowledgements

This work was enabled by the financial support of the Department of Science and Technology, New Delhi under SERC Young Scientist (Anita Mohan) and by RTOP grants from the Solar Physics Office of NASA's Space Physics Division (Roger Thomas). We wish to thank Dr H. E. Mason for helpful comments.

References

Arnaud, M. and Rothenflug, R. : 1985, *Astron. Astrophys. Suppl.* **60**, 425.
Behring, W. E., Cohen, L., Feldman, U., and Doschek, G. A.: 1976, *Astrophys. J.* **203**, 521.
Berrington, K. A.: 1994, *Atomic Data Nuclear Data Tables* **57**, 71.
Brown, J. C., Dwivedi, B. N., Almleaky, Y., and Sweet, P. A.: 1991, *Astron. Astrophys.* **249**, 227.
Dwivedi, B. N.: 1994a, *Space Sci. Rev.* **65**, 289.
Dwivedi, B. N.: 1994b, *Solar Phys.* **153**, 199.
Dwivedi, B. N.: 1996, *Solar Phys.* **165**, 399.
Dwivedi, B. N. and Mohan, A.: 1995a, *Solar Phys.* **158**, 237.
Dwivedi, B. N. and Mohan, A.: 1995b, *Solar Phys.* **156**, 81.
Jordan, C. and Wilson, R.: 1971, in C. J. Macris (ed.), *Physics of the Solar Corona*, D. Reidel Publ. Co., Dordrecht, Holland, p. 219.
Kato, T.: 1994, *Atomic Data Nuclear Data Tables* **57**, 181.
Lang, J. and Summers, H. P.: *Atomic Data Nuclear Data Tables* **57**, 215.
Malinovsky, M. and Héroux, L.: 1973, *Astrophys. J.* **181**, 1009.
Meyer, J. P.: 1985, *Astrophys. J. Suppl.* **57**, 151.
Mohan, A. and Dwivedi, B. N.: 1996, *Solar Phys.* **167**, 145.
Monsignori Fossi, B. C. and Landini, M. : 1994, *Atomic Data Nuclear Data Tables* **57**, 125.
Sampson, D. H., Zhang, H. L., and Fontes, C. J.: 1994, *Atomic Nuclear Data Tables* **57**, 97.
Thomas, R. J. and Neupert, W. M.: 1994, *Astrophys. J. Suppl.* **91**, 461.
Vernazza, J. E. and Reeves, E. M.: 1978, *Astrophys. J. Suppl.* **37**, 485.

Widing, K. G. and Feldman, U.: 1989, *Astrophys. J.* **442**, 446.
Widing, K. G., Feldman, U., and Bhatia, A. K.: 1986, *Astrophys. J.* **308**, 982.
Young, P. R.: 1996, personal communication.
Young, P. R., Landi, E., and Thomas, R. J.: 1998, *Astron. Astrophys.* **329**, 291.
Zhang, H. L., Graziani, M., and Pradhan, A. K.: 1994, *Astron. Astrophys.* **283**, 319.